J Mol Model (2007) 13:121–131
DOI 10.1007/s00894-006-0131-1

ORIGINAL PAPER

Structure-based 3D-QSAR studies on thiazoles as 5-HT_3 receptor antagonists

Li-Ping Zhu · De-Yong Ye · Yun Tang

Received: 2 December 2005 / Accepted: 30 June 2006 / Published online: 5 September 2006

Abstract Structure-based 3D-QSAR studies were performed on 20 thiazoles against their binding affinities to the 5-HT_3 receptor with comparative molecular field analysis (CoMFA) and comparative molecular similarity indices analysis (CoMSIA). The thiazoles were initially docked into the binding pocket of a human 5-HT_{3A} receptor homology model, constructed on the basis of the crystal structure of the snail acetylcholine binding protein (AChBP), using the GOLD program. The docked conformations were then extracted and used to build the 3D-QSAR models, with cross-validated r^2_{cv} values 0.785 and 0.744 for CoMFA and CoMSIA, respectively. An additional five molecules were used to validate the models further, giving satisfactory predictive r^2 values of 0.582 and 0.804 for CoMFA and CoMSIA, respectively. The results would be helpful for the discovery of new potent and selective 5-HT_3 receptor antagonists.

Keywords Structure-based 3D-QSAR · CoMFA · CoMSIA · 5-HT_3 receptor antagonists · Homology modeling

L.-P. Zhu · D.-Y. Ye (✉) · Y. Tang
Department of Medicinal Chemistry, School of Pharmacy,
Fudan University,
138 Yixueyuan Road,
Shanghai 200032, China
e-mail: dyye@shmu.edu.cn

Y. Tang (✉)
School of Pharmacy,
East China University of Science and Technology,
130 Meilong Road,
Shanghai 200237, China
e-mail: ytang234@yahoo.com.cn

Introduction

Nausea and vomiting are major side effects associated with chemotherapy, radiotherapy, and operation [1, 2]. It is now well established that serotonin type 3 (5-HT_3) receptors, present on vagal afferents in the GI tract mucosa and in the brainstem centers, are involved in the vomiting reflex. Initiation of emesis is probably due to the release of serotonin from enterochromaffin cells in the small intestine, which activates vagal afferent nerves via 5-HT_3 receptors [3]. Delayed emesis may involve central 5-HT_3 receptors and/or serotonin stored in the enterochromaffin cells. Specific 5-HT_3 receptor antagonists such as Ondansetron, Granisetron and Tropisetron block nausea and vomiting, probably by competitive inhibition at the 5-HT_3 receptor sites centrally and peripherally [4].

Three subtypes of 5-HT_3 receptors have been identified: (1) 5-HT_{3A}, a neuronal receptor directly coupled to cation-selective channels; (2) 5-HT_{3B}, a regulatory subunit able to modulate the intrinsic channel activity of 5-HT_{3A}; and (3) 5-HT_{3C}, a subunit that appears to modulate the 5-HT_3 receptor responses [5]. The subunit 5-HT_{3A} is functional homo-oligomeric while 5-HT_{3B} is non-functional heteromeric. 5-HT_3 receptors belong to the superfamily of Cys-loop ligand-gated ion channels (LGICs), whose members share significant structural and functional homology to each other. Each subtype consists of five subunits, and each subunit has a large extracellular N-terminal region and four putative transmembrane domains [6, 7]. Early experimental evidence showed that the ligand-binding site is located at the interface of two adjacent subunits. Unfortunately, to date the three-dimensional (3D) structure of 5-HT_3 receptors has not been elucidated, which seriously limits our understanding of the antagonistic mechanism of the receptor in detail. However, the structure of acetylcholine

Scheme 1 Structures and actual pKi values of molecules used for 3D-QSAR studies [12, 13]

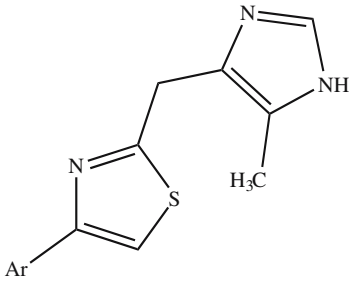

1-19

Ar

1. Indol-3-yl (7.921)
2. *o*-$MeOC_6H_4$ (9.377)
3. C_6H_5 (8.745)
4. Quinolin-8-yl (9.000)
5. *o*-FC_6H_4 (8.712)
6. *o*-$EtOC_6H_4$ (9.022)
7. *o*-HOC_6H_4 (8.824)
8. *o*-MeC_6H_4 (8.061)
9. *m*-ClC_6H_4 (9.056)
10. *m*-$MeOC_6H_4$ (8.699)
11. *m*-FC_6H_4 (8.432)
12. *m*-BrC_6H_4 (8.699)
13. *p*-FC_6H_4 (8.310)
14. *p*-MeC_6H_4 (6.959)
15. *p*-BrC_6H_4 (6.569)
16. *p*-ClC_6H_4 (7.469)
17. 1-Methoxynaphth-2-yl (7.022)
18. 2-Methoxynaphth-1-yl (6.398)
19. 2,6-$(MeO)_2C_6H_3$ (6.367)

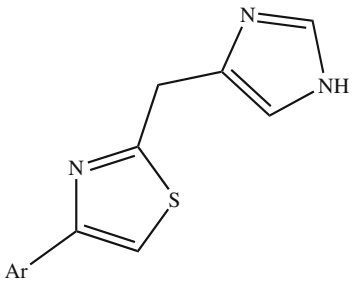

20-23

Ar

20. C_6H_5 (9.000)
21. *o*-$MeOC_6H_4$ (9.538)
22. Quinolin-8-yl (9.509)
23. Indol-3-yl (7.848)

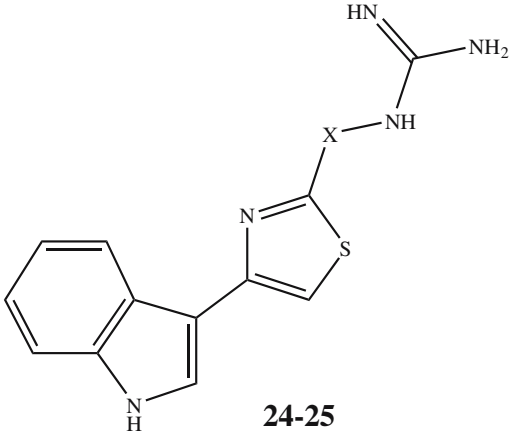

24-25

X

24. CH_2 (8.481)
25. $COOCH_2CH_2$(8.149)

binding protein (AChBP) found in the snail *Lymnaea stagnalis* has been determined by X-ray crystallography. This protein is a member of the LGICs, and shares 19% homologous sequence with the extracellular domain of the 5-HT_{3A} receptor [8]. Therefore, a homology model of the extracellular domain of the human 5-HT_{3A} receptor was built based on the crystal structure of AChBP, and known selective antagonists were docked into the binding site to validate the model. During the course of this work, a similar study using a range of antagonists was published [9].

QSAR and 3D-QSAR have long been used to elucidate the mechanisms of drug action and for lead optimization. CoMFA (comparative molecular field analysis) [10] and CoMSIA (comparative molecular similarity indices analysis) [11] are two of the most widely used 3D-QSAR methods. In both approaches, molecular property fields are evaluated between a probe atom and each molecule of a dataset at the intersections of a regularly spaced grid. CoMFA calculates steric and electrostatic properties according to Lennard-Jones and Coulomb potentials, while CoMSIA considers five different similarity fields: steric, electrostatic, hydrophobic, hydrogen-bond donor, and hydrogen-bond acceptor properties. When the 3D-structure of a receptor is also available, ligand- and structure-based drug design methods can be combined. The structure-based 3D-

Scheme 2 Sequence alignment of the extracellular domain of human 5-HT_{3A} receptor subunit with that of AChBP. The crystal structure of AChBP was taken from the PDB file (1I9B). Secondary structure elements of AChBP (α-helix, red; β-strand, blue; 3_{10}-helix, green) were indicated [8]

QSAR method is the result of such a combination, and it could provide more information for lead optimization.

In order to understand the antagonistic mechanism and guide the discovery of more potent ligands, a series of highly potent and selective 5-HT_3 receptor antagonists, reported by Nagel et al. [12, 13] were chosen to perform 3D-QSAR studies with both CoMFA and CoMSIA methods, based on their docking conformations on the structural model of human 5-HT_{3A} receptor in this paper. The molecules chosen contain a thiazole moiety linking an aromatic group and a nitrogenous basic region (Scheme 1); the thiazole group appears to be acting as a carbonyl bioisostere in this system. By mapping the CoMFA and CoMSIA contour plots onto the structural model of the receptor, the results of this study might be conversely validate the 3D-structural model of the receptor.

Materials and methods

Sequence alignment

The sequence alignment of the extracellular domain of human 5-HT_{3A} receptor with AChBP is shown in Scheme 2 [8].

Dataset

Twenty-five thiazoles were collected from literature reported by Nagel [12, 13]. The binding affinities of these compounds to the 5-HT_3 receptor were evaluated with replacement of [^{3}H]-Tropisetron binding to NG-108-15 cells. The compounds were divided into two sets: 20 molecules selected randomly to form the training set, whereas the remaining five molecules served as an external test set.

Molecular modeling

All molecular modeling studies were carried out on an R14000 SGI Fuel workstation using the molecular modeling software package SYBYL v6.9 [14]. The three-dimensional model of the extracellular region of human 5-HT_{3A} receptor was built using the module BIOPOLYMER based on the crystal structure of AChBP determined at 2.7 Å (PDB entry code: 1I9B) [8]. The pentamer was generated by replacing each amino acid of AChBP with the corresponding one of human 5-HT_{3A} receptor's extracellular regions, ensuring the conformation of the template's backbone unchanged. The model generated was fixed using the Biopolymer command Fix Proline and Fix Sidechains, to relieve all bad van der Waals contacts. Then the model was minimized using the AMBER4.1 force field [15] with a distance-dependent dielectric constant of 5.0 and a gradient convergence value of 0.05 kcal mol^{-1} in 2,000 cycles. Atomic charges were calculated using the AMBER4.1 method. Then subunit A and B were extracted and used as the initial model for further docking studies. Sixteen 5-HT_3 receptor antagonists, known as 'setrons', were docked into the binding pocket of the initial model, and the residues within 10 Å of the ligand of the ligand-receptor complex were minimized. Finally, the model was validated

by PROCHECK and Verify_3D (http://nihserver.mbi.ucla.edu/SAVS/, [16]).

The 16 setrons, compounds **2** and **24** were retrieved from the MDDR database from MDL (http://www.mdli.com). The 2D-structures were subsequently converted into 3D-structures with CORINA (http://www2.ccc.uni-erlangen.de/software/corina/free_struct.html). All the other 23 compounds were constructed based on the structure of compound **2**. All molecules were set in their unprotonated state and Gasteiger–Hückel charges were added in SYBYL.

Ligand docking

The binding site of the 5-HT_3 receptor was defined as atoms within a radius of 16 Å of the C_α atom of Trp178 in the binding pocket to ensure that most of the residues critical for ligand binding verified/revealed by previous experimental data were included. All molecules were docked into the binding pocket with the program GOLD v2.2 [17–19]. The default settings of GOLD were used, and no flipping was allowed.

CoMFA and CoMSIA

First, the docked conformations of the molecules in the training set were placed into a 3D cubic lattice with 2 Å grid. CoMFA fields were generated using an sp^3 carbon probe atom carrying +1 charge to generate steric (Lennard-Jones potential) and electrostatic (Coulomb potential) fields at each grid point. The CoMFA fields were scaled by the CoMFA-Standard method in SYBYL. A 30 kcal mol^{-1} energy cutoff was applied.

The steric, electrostatic, hydrophobic, hydrogen-bond donor and acceptor CoMSIA fields were derived according to Klebe et al. [10]. A distance-dependent Gaussian type functional form was used. The default value of 0.3 was used as the attenuation factor. Similar to CoMFA, a data table was constructed from similarity indices calculated at the intersections of a regularly spaced lattice (2 Å grid) in CoMSIA.

PLS analysis and validation of QSAR models

The CoMFA/CoMSIA fields combined with observed biological activities (pK_i) were included in a molecular spreadsheet, and partial least square (PLS) methods [20] were used to generate 3D-QSAR models. To check the statistical significance of the models, cross-validations were done to choose the optimum number of components (N) by means of the leave-one-out (LOO) [21] procedure using the enhanced version of PLS, the SAMPLS method [22], subsequently used to derive the final QSAR models. The optimal numbers of components were selected on the basis of the highest cross-validated correlation coefficient $\left(r^2_{cv}\right)$, which is defined as follows:

$$r^2_{cv} = -\frac{\sum \left(Y_{predicted} - Y_{actual}\right)^2}{\Sigma \left(Y_{actual} - Y_{mean}\right)^2} \quad (1)$$

Where $Y_{predicted}$, Y_{actual}, and Y_{mean} are predicted, actual, and mean values of the target property (pK_i), respectively. The non-cross-validated PLS analyses were performed with a column filter value of 2.0. The CoMFA/CoMSIA results were interpreted graphically by field contribution maps using the 'STDEV×COEFF' field type.

To assess the predictive power of the 3D-QSAR models derived using the training set, biological activities of the test set molecules were predicted. The predictive $r^2\left(r^2_{pred}\right)$ value is calculated as follows:

$$r^2_{pred} = (SD - PRESS)/SD$$

Where SD is the sum of squared deviations between the biological activity of the test set and the mean activity of training-set molecules, and PRESS is the sum of squared

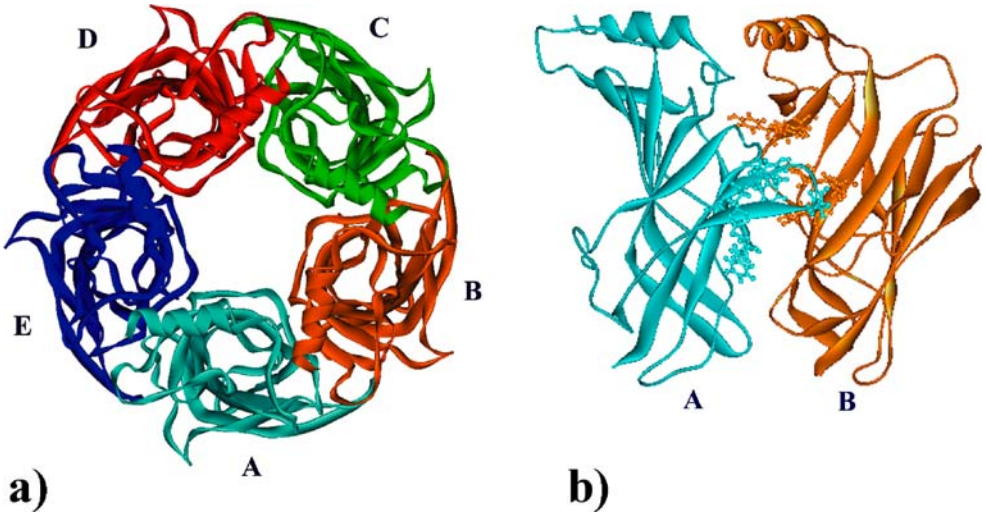

Fig. 1 (**a**) Overview of the pentameric structure of the initial model. In this presentation each monomer has a different color. Subunits are labeled anti-clockwise, with A-B, B-C, C-D, D-E and E-A forming the plus and minus interface side. (**b**) Details of ligand binding site, especially the residues approved to be important for ligands binding (ball-and-stick representation), are shown in the A and B interface of the model

Table 1 5-HT_3 receptor antagonists selected for docking studies

Group A	Group B
Alosetron	Azasetron
Cilansetron	Bemesetron
Dolasetron	Granisetron
Fabesetron	Indisetron
Galdansetron	Palonosetron
Lurosetron	Ramosetron
Ondansetron	Ricasetron
Tropisetron	Zatosetron

deviations between the actual and the predicted activities of the test set molecules. In addition, the r^2_{cv}, r^2_{pred} and number of components, the conventional correlation coefficient r^2 and its standard error were also computed for each model.

Results and discussion

Sequence identity of the extracellular region of human 5-HT_3 receptor with AChBP is about 19%. When the conservative replacements are considered, their sequence homology is beyond 30%, which could result in at least 80% identity with the secondary structure of AChBP [9]. Homology modeling resulted in a β-sandwich structure (Fig. 1) similar to that of AChBP.

Ligand docking and validation of the model

Sixteen selective 5-HT_3 receptor antagonists were docked into the binding pocket of the initial model. The setrons reported to date may be expressed with such a pharmacophore: a carbonyl-containing side chain flanked by a lipophilic aromatic group and a nitrogenous basic moiety [23]. As mentioned above, a similar study using a range of antagonists was published, which suggested that the aromatic groups of antagonists were supposed to intercalate between aromatic side-chains of the receptor (Trp178–Tyr229, Tyr138–Tyr148); while the basic centers interact with Glu231 or Glu124 (ionic interaction), and/or Trp85 (cation–π interaction) of the receptor [9].

In our study, the docking conformations with highest score of setrons (one per setron) fell broadly into two groups, which we have designated A and B (Table 1). However, the observations fitted the result recently published by Lummis et al. [24]. In group A, the azabicyclic ring of setrons was located between Trp178 and Tyr229, and the aromatic rings lay near Phe221. In group B, the orientation of setrons was reversed, and consequently the aromatic rings was located between Trp178 and Tyr229, and the azabicyclic ring lay near Phe221. Representatives from each group are shown in Fig. 2.

The final model was validated by PROCHECK and Verify_3D. The results are shown in Fig. 3. 75.9% of the residues were located in the darkest 'core' regions (marked A, B, and L) in the Ramachandran Plot, which fitted the majority of PDB (72.9% in most favored regions for 2.7 Å X-ray structures) [25]. As for the Verify_3D results, 71.70% of the final model residues had an averaged 3D–1D score >0.2, while the initial model showed 62.26% of the residues had an averaged 3D–1D score >0.2. Above all, the model could be accepted for further studies.

Twenty-five molecules extracted from Nagel et al. were docked into the binding pocket of the final model. Conformations (one per compound) were selected manually in 3D-QSAR analysis, considering both the docking score and the conformation reliability (Fig. 4). The superposition showed reasonable fit to the binding pocket consisting of residues that had been proven to be critical for ligand binding. The imidazole ring of most ligands seemed to form π–π interactions with Trp85, Trp178 and Tyr229 of the receptor. The NH moiety of the imidazole ring of most ligands donated hydrogen bonds to Tyr148 and Trp178 of the receptor. However, these observations differed from

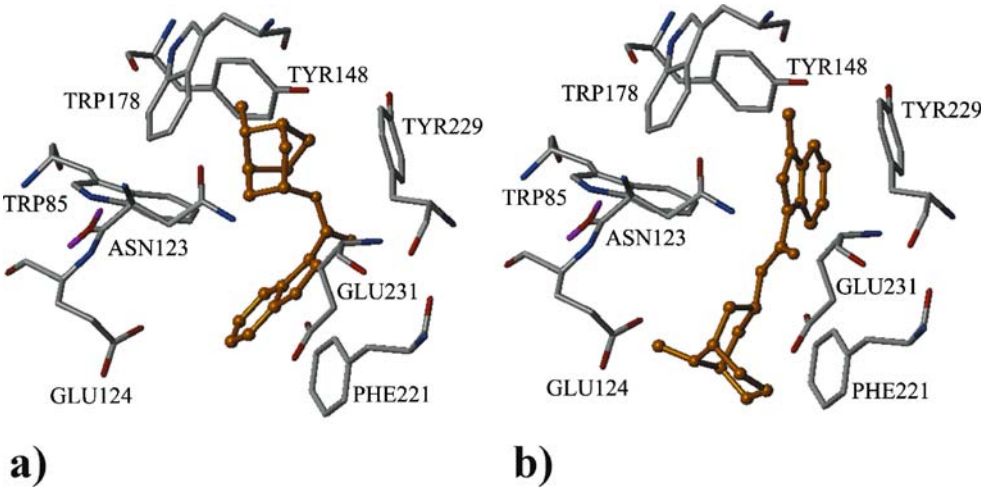

Fig. 2 (**a**) The docked conformation of Tropisetron together with the binding site of human 5-HT_{3A} receptor, as is the case of setrons in Group A, which was above-mentioned in the paper. (**b**) The docked conformation of Granisetron together with the binding site of human 5-HT_{3A} receptor, as is the case of setrons in Group B. The ligand is shown in orange (ball-and-stick representation). (All hydrogen atoms were omitted for a better view)

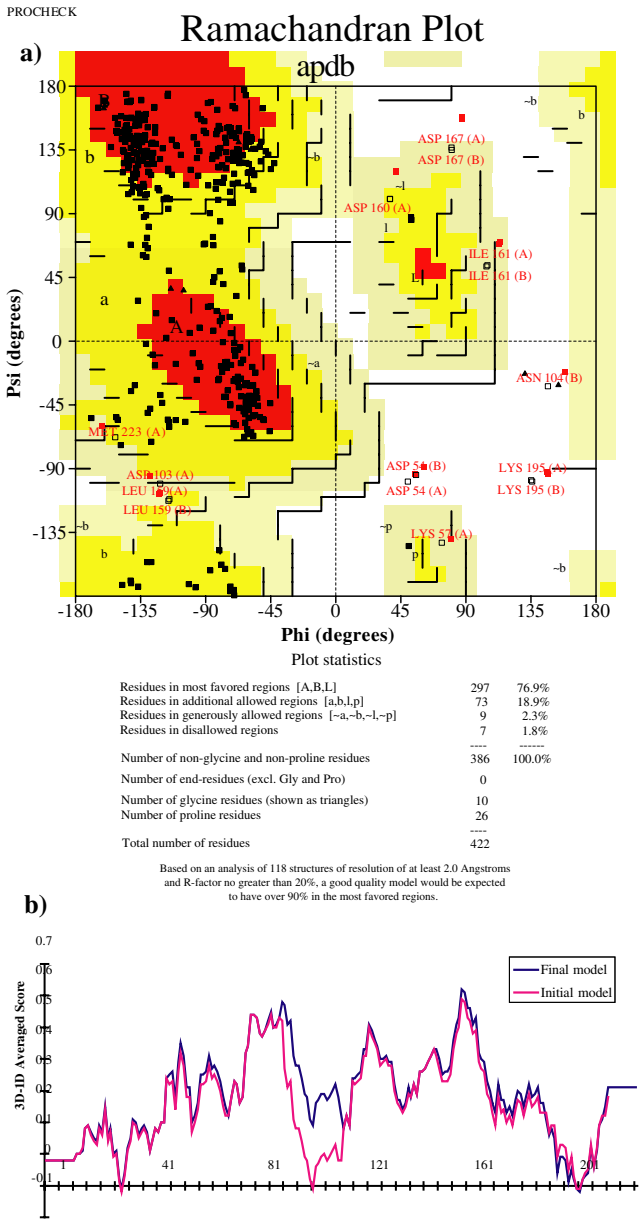

Fig. 3 (**a**) The Ramachandran plot of the final model produced by PROCHECK. (**b**) Profile window plots for the initial and final models resulted from Verify_3D. The vertical axis gives the average 3D-1D score for residues. The conformation of the residues which have got a bad score needs to be adjusted

above-mentioned Groups A and B, and thus might reveal a novel interaction mode between 5-HT_3 receptor and antagonists. On the other hand, the results of the docking studies and 3D-QSAR would offer constructive suggestions to the further rectification of the receptor model.

CoMFA

The CoMFA result is summarized in Table 2. The cross-validated value, r^2_{cv}, is 0.785, with an optimum number of components 6. The non-cross-validated PLS analysis

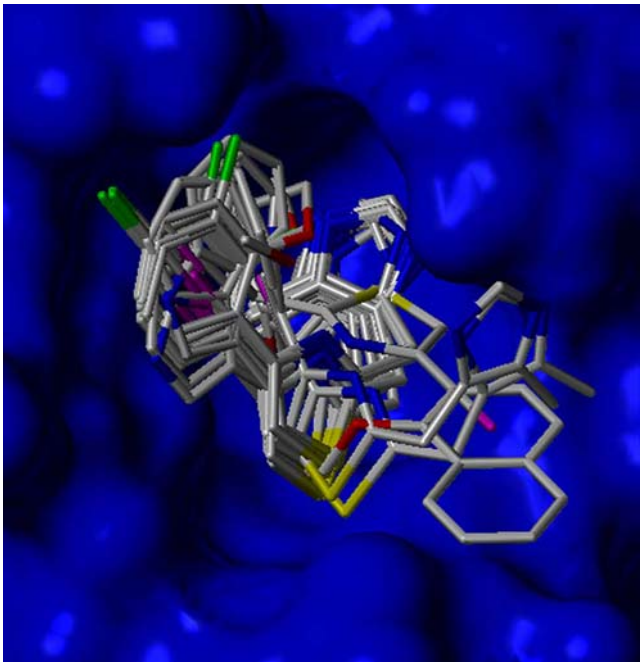

Fig. 4 The docked conformations of 20 molecules in the training set together with the binding site of human 5-HT_{3A} receptor. The solvent-accessible surface is indicated as a solid surface. (All hydrogen atoms were omitted.)

produced an r^2 of 0.986. These statistical indices were reasonably high, indicating that the CoMFA model might have a strong predictive ability. The predicted affinities and the residual values of the training set and the test set are given in Table 3.

The steric field descriptor explained 62.2% of the variance, and the proportion of electrostatic descriptor accounted for 37.8%. Therefore, the steric field had greater influence than the electrostatic field. The CoMFA contours were mapped into the ligand-receptor complex structure (Fig. 5).

Table 2 Summary of results from the CoMFA and CoMSIA analysis

	r^2_{cv} [a]	N[b]	r^2[c]	SEE[d]	F[e]
CoMFA	0.785	6	0.986	0.148	156.212
CoMSIA (S+E)	0.559	2	0.705	0.600	20.293
CoMSIA (S+E+H)	0.796	4	0.934	0.303	52.909
CoMSIA (S+E+H+D)	0.739	5	0.936	0.308	40.960
CoMSIA (S+E+H+A)	0.761	5	0.939	0.301	42.975
CoMSIA (S+E+H+D +A)	0.744	5	0.934	0.312	39.761

S, *E*, *H*, *D*, and *A* represent the steric, electrostatic, hydrophobic, hydrogen bond donor and acceptor property fields, respectively
[a] Leave one out (LOO) cross-validation correlation coefficient
[b] Optimum number of components
[c] Non-cross-validation correlation coefficient
[d] Standard error of estimate
[e] *F*-test value

Table 3 Experimental pK_i, predicted pK_i and residual values of molecules used in the training set and test set for CoMFA and CoMSIA

		Predicted pK_i		Residual values	
Compd	Actual pK_i	CoMFA	CoMSIA	CoMFA	CoMSIA
Training set					
2	9.377	9.373	9.270	0.004	0.107
3	8.745	8.454	8.353	0.291	0.392
5	8.712	8.901	8.781	−0.189	−0.069
6	9.022	8.993	9.318	0.029	−0.296
8	8.061	8.344	8.346	−0.283	−0.285
9	9.056	8.974	8.725	0.082	0.331
11	8.432	8.433	8.617	−0.001	−0.185
12	8.699	8.784	9.034	−0.085	−0.335
13	8.310	8.233	7.967	0.077	0.343
14	6.959	6.994	7.605	−0.035	−0.646
15	6.569	6.650	6.654	−0.081	−0.085
16	7.469	7.377	7.233	0.092	0.236
17	7.022	6.992	7.095	0.030	−0.073
18	6.398	6.342	6.430	0.056	−0.032
19	6.367	6.430	6.272	−0.063	0.095
20	9.000	8.931	8.641	0.069	0.359
21	9.538	9.637	9.383	−0.099	0.155
22	9.509	9.393	9.563	0.116	−0.054
23	7.848	7.784	7.819	0.064	0.029
24	8.481	8.557	8.469	−0.076	0.012
Test set					
1	7.921	7.871	7.822	0.050	0.099
4	9.000	8.926	8.809	0.074	0.191
7	8.824	8.752	8.560	0.072	0.264
10	8.699	9.283	8.846	−0.584	−0.147
25	8.149	8.185	8.321	−0.036	−0.172

The steric contour map (Fig. 5a) showed a green region surrounding the C-2,3 position of the phenyl ring (Scheme 3), indicating that a bulky substituent is preferred to produce higher activity, which was consistent with the experiments that hydroxylated thiazoles were generally less active than their alkoxylated counterparts. However, it seemed that this region collided slightly with Glu224 and Ser225 of the 5-HT_{3A} receptor, which meant the size of substituent was not unlimited, otherwise it would encounter the receptor. There was another green region near the C-5' position of the imidazole ring, which could explain why compound **1** was more active than **23**. The yellow steric contour near the C-4 position of the phenyl ring indicated that any bulky substituent decreased activity, which should account for the activity differences of 4-halogenated thiazoles: **13**(F-, 8.310), **16**(Cl-, 7.469) and **15**(Br-, 6.569).

The CoMFA electrostatic contour plot is shown in Fig. 5b. There were two minor blue regions near the C-2 position of the phenyl ring and the C-5' position of the imidazole ring, the former of which was located between Tyr148 and Tyr229 of the 5-HT_{3A} receptor, indicating that substitution of electropositive group at this position would increase the activity. This is why compound **18** as well as **19**, whose OCH_3 group was around the blue region, have low activity. The presence of a red contour near the N-1' atom of the imidazole ring corresponding to Trp178 of the receptor emphasized that an electronegative group is desirable at this position. Compounds occupying both blue and red contours showed moderate activities, such as **23** and **24**.

CoMSIA

The results of CoMSIA are shown in Table 2. The CoMSIA model including S, E and H performed better than the other field combinations. The CoMSIA model that included all five fields was chosen for further analysis, as it would provide comprehensive information especially when the receptor was concerned. The contributions were 10.3, 21.3, 33.0, 20.1 and 15.3% for S, E, H, D, and A, respectively. The calculated activities and the residual values predicted by the CoMSIA model for the training set and the test set are given in Table 3.

The steric field contour plots are shown in Fig. 6a. There is a major white region around the C-2,3 positions of the phenyl ring and a minor yellow steric contour near the C-4 position, which indicates that a large group around the C-2,3 positions and a small group near the C-4 position would be beneficial to the binding affinity. This is supported by the relatively higher affinities of compound **2**, **6**, **9**, **11** and lower affinities of **14**, **15**, and **16** than compound **3**.

The CoMSIA electrostatic field contour plots are shown in Fig. 6b. White areas, positive charges favorable to affinity, corresponding to Tyr229 of the receptor, spread around the thiazole and imidazole ring. Compounds **18** and **19** oriented their atom-N into the disfavored regions, shown in white, resulting in bad binding affinity. The small yellow region near the C-2 position of the phenyl ring indicates that electronegative groups at this position may enhance the activity. Therefore, the activity of **2** was about ten-fold higher than that of **8**, in which the $–OCH_3$ group replaced the $–CH_3$ group.

The hydrophobic contours are shown in Fig. 6c. The white hydrophobic contour near the C-2,3 position of the phenyl ring matches the green steric contour (Fig. 6a). This indicates that any bulky group with lipophilic character is preferred at this position. The result agrees with the contours of the CoMSIA steric field. The less active **18** and **19** orient their OCH_3 into the white contoured region, whereas the more active **8** occupies the favored area with its methyl substituent. The yellow hydrophilic contour near the C-4 position indicates that any lipophilic group at this position decreases the activity. Thus, the activity of molecule with F (**13**) or Cl (**16**) at this position is higher

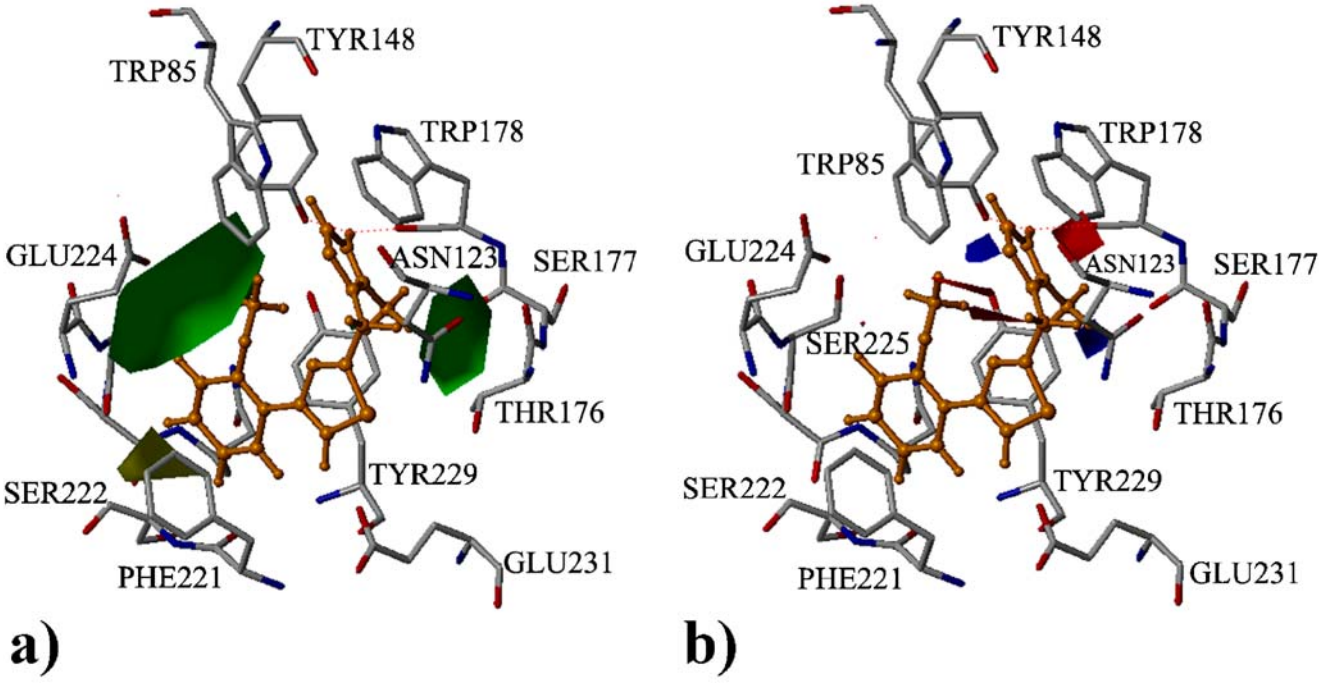

Fig. 5 Mapping the CoMFA contours in the active site of 5-HT_{3A} receptor with compound 2 as an example. The hydrogen bonds are shown in broken red lines. The ligand is shown in orange. The contour plots (STDEV*COEFF) of the CoMFA: (**a**) steric fields; green contours indicate regions where bulky groups increase activity, whereas yellow contours indicate regions bulky groups decrease activity and (**b**) electrostatic fields; blue contours indicate regions where electropositive groups increase activity, whereas red contours indicate regions where electronegative groups increase activity. (All hydrogen atoms of the receptor were omitted)

than that of the molecule with a CH_3 (**14**) group. There were several molecules for which the activities could not be interpreted by the hydrophobic contours alone. For example, the affinities of compounds **9**, **11** and **12** should be bad due to the halogen substituent near the white contoured area. In fact, their activities are moderately high. All of the five fields' properties may be needed to describe the case.

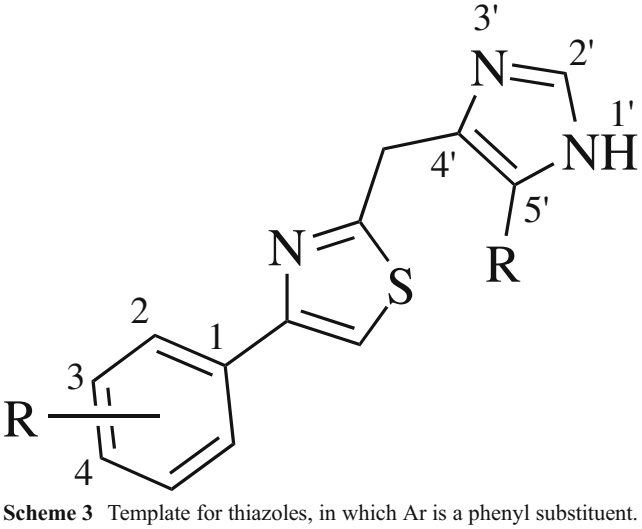

Scheme 3 Template for thiazoles, in which Ar is a phenyl substituent. Note that the atom numbering does not follow the IUPAC rules

As for the receptor, the white contours should correspond to the hydrophobic residues, whereas the yellow ones should be near the polar residues. Actually, the major white as well as the yellow contour are opposite Glu224 and Ser225, while the minor white contour faces Trp178. We suggest that the position of Glu224 and Ser225 might be rectified.

The hydrogen-bond donor and acceptor contours are shown in Fig. 7a,b, respectively. The presence of cyan-colored contour near the NH group of the imidazole ring indicates that a corresponding hydrogen bond acceptor on the 5-HT_{3A} receptor might exist. This is consistent with the fact that most ligands form hydrogen bonds with Tyr148 and Trp178. Molecules occupying the cyan contour with their NH group (**2** and **22**) revealed high affinities, whereas those orienting their donor into the disfavored regions (**18** and **19**) showed low affinities. Furthermore, molecules possessing both cyan and purple contours were moderately active, such as **23** and **24**.

Two magenta regions near N and O implied that hydrogen-bond donors may exist at the corresponding positions of the receptor's active site (Trp85, Tyr148 and Tyr229), consistent with our homology model. This observation clearly indicates that a hydrogen-bond acceptor near the magenta contours would increase the activity. The NH group and N atom of the imidazole ring at these

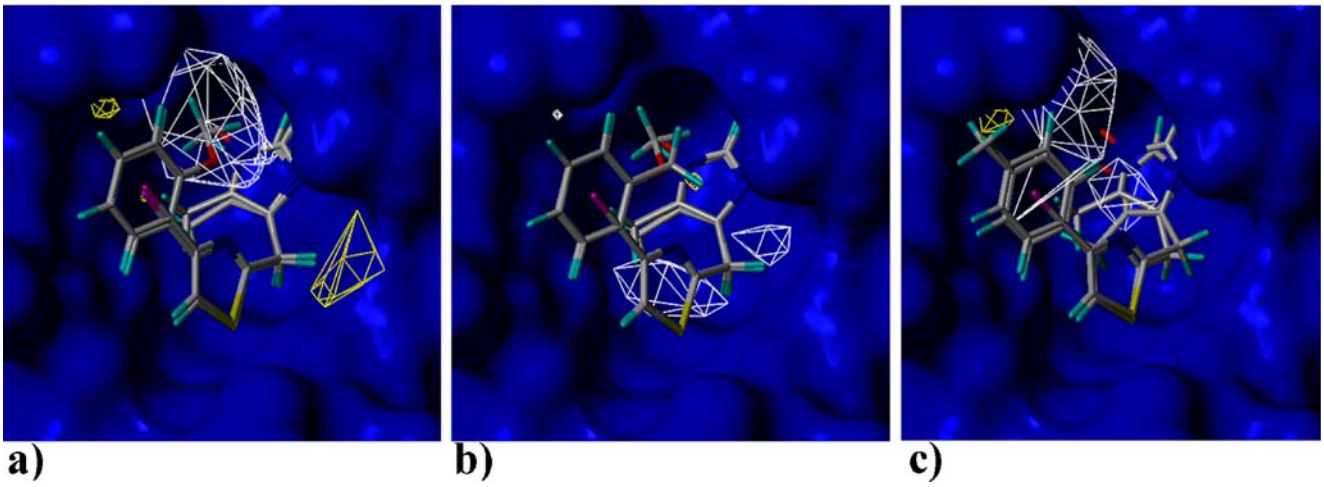

Fig. 6 Contour plot of the CoMSIA stdev*coeff for (**a**) steric features: White isopleths enclose areas where steric bulk will enhance affinity, Yellow contours highlight areas which should be kept unoccupied; (**b**) electrostatic properties: White isopleths encompass regions where an increase of positive charge will enhance affinity, whereas in yellow contoured areas more negative charges are favorable for binding properties; (**c**) hydrophobic properties: White isopleths encompass regions favorable for hydrophobic groups, whereas in yellow contoured areas more hydrophilic groups are favorable for binding properties. The solvent-accessible surface is indicated as a solid surface

two positions were present in all these molecules. A red contour of hydrogen bond acceptor near C-2 position of the phenyl ring indicates that molecules with hydrogen bond acceptor at this position would be less active, such as **15**, **17**, **18** and **19**.

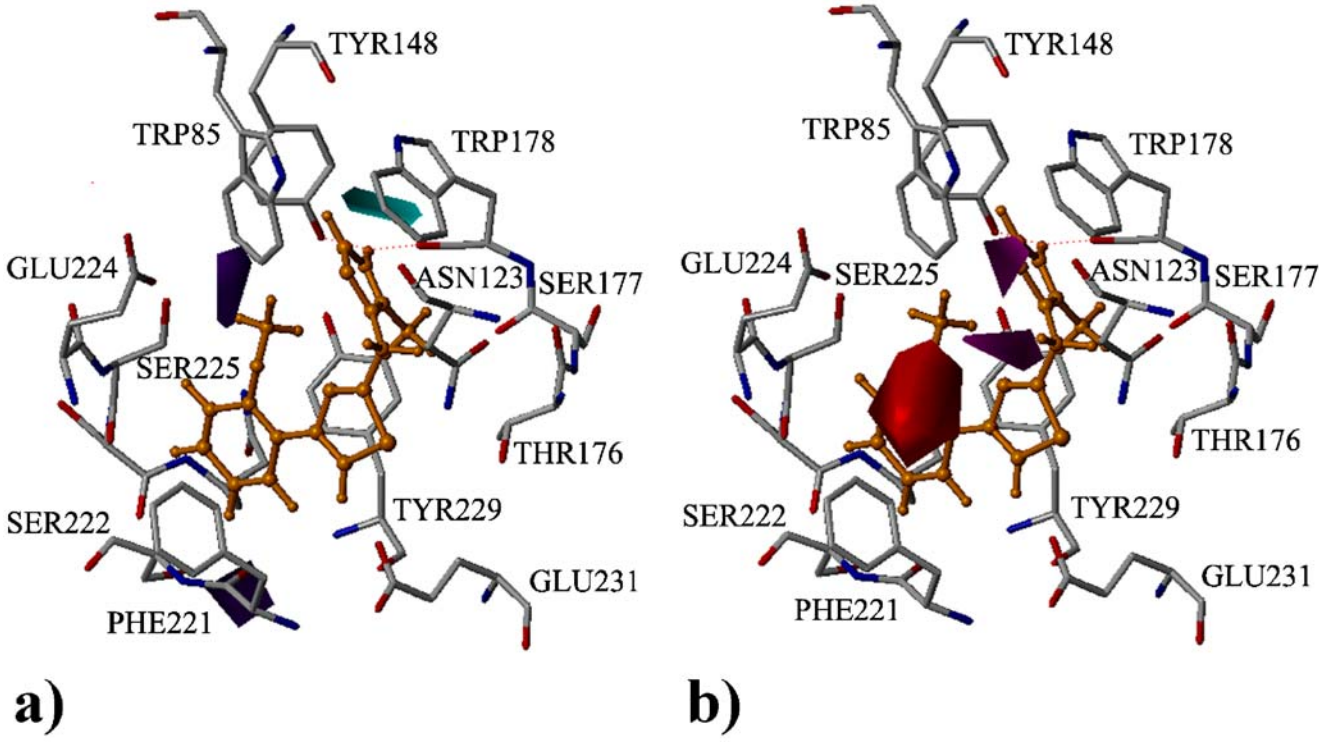

Fig. 7 Mapping the CoMSIA contours in the active site of 5-HT_{3A} receptor with compound 2 as an example. The hydrogen bonds are shown in broken red lines. The ligand is shown in orange. The contour plots (STDEV*COEFF) of the CoMSIA: (**a**) donor fields (the presence of cyan-colored contour correspondes to hydrogen bond acceptor on the receptor, as leads to higher activity, whereas purple contoured areas are unfavorable for binding properties), (**b**) acceptor fields (magenta isopleths encompass regions containing hydrogen bond acceptor which interacts with hydrogen bond donor on the receptor, whereas red contoured areas are disfavored). (All hydrogen atoms of the receptor were omitted)

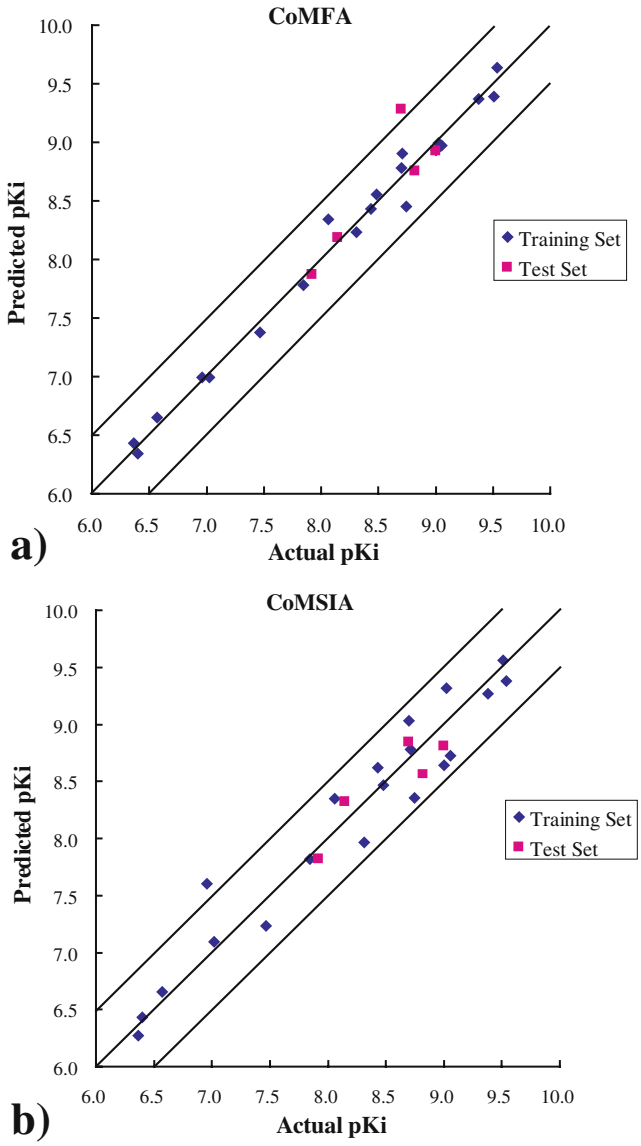

Fig. 8 Actual versus predicted pKi of training and test set molecules for (**a**) CoMFA and (**b**) CoMSIA 3D-QSAR models. The predicted values fell close to the observed pKi values, deviating by not more than 0.5 logarithmic units mostly

Validation of 3D-QSAR models

The predictive power of the CoMFA and CoMSIA 3D-QSAR models was evaluated further by five additional molecules in the test set. The results showed that a moderately bulky hydrophobic substituent (i.e. OCH_3, OCH_2CH_3, and $NHCH_3$) at the C-2,3 positions and a small hydrophilic group (i.e. OH, NH_2) at the C-4 position of the phenyl ring were preferred to produce higher binding affinities. The activities of corresponding pyridyl derivatives, in which an N atom replaced C-4, were also theoretically high. The set of compounds is worthy of further studies.

Figure 8 shows the plots of actual versus predicted activity for both training set and test set. In almost all cases of 3D-QSAR models, the predicted values fall close to the observed pK_i values, deviating by not more than 0.5 logarithmic units except for compound **10**. Finally, CoMFA and CoMSIA possessed distinct predictive power with respect to these five compounds (0.582 vs. 0.804).

Summary

In this study, CoMFA and CoMSIA 3D-QSAR analyses were carried out on the docked conformations of 25 thiazoles as 5-HT_3 receptor antagonists with the original intention to validate the 3D-model of the extracellular domain of the human 5-HT_{3A} receptor. The QSAR models may have good prediction capability in terms of r^2_{cv} and r^2 values. The well-correlated 3D-QSAR models showed that it is reliable to construct the models on the docking conformations, which are close to pharmacophoric conformations. The effects of the steric, electrostatic, hydrophobic, and H-bond donor and acceptor fields around the docked conformations on their affinities were discussed in detail. According to these studies, some implications could be drawn to improve the activity and selectivity of thiazoles as 5-HT_3 receptor antagonists, for example, moderately bulky hydrophobic substituent at the C-2,3 position and small hydrophilic group at the C-4 position of the phenyl ring were preferred to produce higher activity. Besides, the replacement of C-4 atom by N atom would result in comparative affinities theoretically. The results of 3D-QSAR were also consistent with the docking studies, which provided a tool to predict the affinity of related thiazoles, and to guide further structural modification and synthesis of new potent and selective 5-HT_3 receptor antagonists. Syntheses of new derivatives designed based on the 3D-QSAR results are in progress.

References

1. Wolf H (2000) Scand J Rheumatol 29:37–45
2. Haus U, Spath M, Farber L (2004) Scand J Rheumatol 33:12–18
3. Karim F, Roerig SC, Saphier D (1996) Biochem Pharmacol 52:685–692
4. Israili ZH (2001) Curr Med Chem—Central Nervous System Agents 1:171–199
5. Lummis SCR, Reeves DC (2002) Mol Membrane Biol 19:11–26
6. Boess FG, Beroukhim R, Martin IL (1995) J Neurochem 64:1401–1405
7. Boess FG, Steward LJ, Steele JA, Liu D, Reid J, Glencorse TA, Martin IL (1997) Neuropharmacol 36:637–647
8. Brejc K, Van Dijk WJ, Klaassen RV, Schuurmans M, van der Oost J, Smit AB, Sixma TK (2001) Nature 411:269–276
9. Maksay G, Bikádi Z, Simonyi MJ (2003) Recept Signal Transduct Res 23:255–270

10. Cramer III RD, Patterson DE, Bunce JD (1998) J Am Chem Soc 110:5959–5967
11. Klebe G, Abraham U, Mietzner T (1994) J Med Chem 37: 4130–4146
12. Rosen T, Nagel AA, Rizzi JP, Ives JL, Daffeh JB, Ganong AH, Guarino K, Heym J, McLean S, Nowakowski JT, Schmidt AW, Seeger TF, Siok CJ, Vincent LA (1990) J Med Chem 33: 2715–2720
13. Nagel AA, Rosen T, Rizzi J, Daffeh J, Guarino K, Nowakowski J, Vincent LA, Heym J, McLean S, Seeger T, Connolly M, Schmidt AW, Siok C (1990) J Med Chem 33:13–16
14. SYBYL, version 6.9. (2004) Molecular Modeling Software, Tripos Associates Inc, 1669, South Hanley Road, Suite 303, St. Louis, Missouri, MO 63144–2913, USA
15. Pearlman DA, Case DA, Kollman PA (2004) AMBER 4.1. University of California, San Francisco, CA
16. Laskowski RA (1993) J Appl Cryst 26:283–291
17. GOLD, version 2.2. (2004) CCDC Software Ltd, 12 Union Road, Cambridge CB2 1EZ, United Kingdom, http://www.ccdc.cam.ac.uk
18. Jones G, Willett P, Glen RC, Leach AR, Taylor R (1997) J Mol Biol 267:727–748
19. Jones G, Willett P, Glen RC (1995) J Mol Biol 245:43–53
20. Wold S, Ruhe A, Wold H, Dunn III WJ (1984) SIAM J Sci Stat Comput 5:735–743
21. Cramer III RD, Bunce JD, Patterson DE (1988) Quant Struct-Act Relat 7:18–25
22. Bush BL, Nachbar Jr RB (1993) J Comput-Aided Mol Des 7: 587–619
23. Hibert MF, Hoffmann R, Miller RC, Carr AA (1990) J Med Chem 33:1594–1600
24. Thompson AJ, Price KL, Reeves DC, Chan SL, Chau PL, Lummis SCR (2005) J Biol Chem 280:20476–20482
25. Pontius J, Richelle J, Wodak SJ (1996) J Mol Biol 264:121–136